JOURNAL OF SOLID STATE CHEMISTRY 19, 35–44 (1976)

The Crystal Structure of Rb–β-Alumina

TOSHIKO KODAMA AND GIICHI MUTO

The Institute of Industrial Science, The University of Tokyo, 22-1, Roppongi 7-chome, Minato-ku, Tokyo 106, Japan

Received March 23, 1976

The crystal structure of $Rb_2O \cdot 11Al_2O_3$ has been determined from three-dimensional X-ray data. The compound forms hexagonal crystals with $a = 5.600$, $c = 22.87$ Å, and $Z = 1$ in space group $P6_3/mmc$. The structure has been refined by least-squares methods with anisotropic temperature factors to an R value of 0.079 for 331 independent reflections collected by diffractometry. The mobile ion sites and their occupation percentages are discussed in relation to other β-alumina compounds. The covalently bonded corner-sharing $O_3Al–O–AlO_3$ tetrahedra are discussed in relation to the ionic conduction phenomena.

Introduction

β-Alumina compounds have a unique character for their two-dimensional ionic conductivities over a wide temperature range and have the conduction plane of rather simple structures, consisting of a mobile ion and an oxygen ion. Furthermore, β-alumina compounds exchange mobile ion species with each other easily in their molten salt (*1*). Thus, the ionic conductivity of β-alumina compounds can be studied by selecting the mobile ion species as a parameter.

The crystal structure of Tl–β-alumina (*2*) has been studied previously to clarify the change of structure when the conduction layer was varied in space by the thallium ion. Several kinds of available lattice points for the mobile ion were observed more clearly in Fourier maps in comparison with those of Ag– and Na–β-alumina (*3*, *4*). We selected the rubidium ion, which has a strong ionic character and is large in size, and investigated the crystal structure of Rb–β-alumina by the X-ray crystal structure analysis method in order to clarify the character of the available lattice sites for the mobile ion.

Experimental

Samples of Rb–β-alumina were prepared from crystals of Na–β-alumina by immersing them in excess pure molten salt of rubidium nitrate using the same process as with that of Tl–β-alumina (*1*, *2*). Crystals of Na–β-alumina were kindly supplied by Dr. Atuo Imai and Dr. Mituo Harata of Toshiba Research and Development Center of Tokyo Shibaura Electric Co. The ion exchange process was observed by the weight change of each of samples. The total immersion time, about 700 hr, was quite sufficient for ion exchange.

Crystals are colorless and transparent. They cleave easily to thin plates perpendicular to the c-axis, but it is rather difficult to cut them in the c-plane. The crystal density was determined by floating a crystal in a thallium formate–water mixture.

Crystal Data

General formula: $Rb_2Al_{22}O_{34}$
F. W. = 1360
Hexagonal
$a = 5.600(1)$ Å
$c = 22.87(1)$ Å

$Z = 1$
$V = 621.0(1)$ Å^3
$D_x = 3.57$ g·cm^{-3}
$D_m = 3.3(2)$ g·cm^{-3}
Systematic absences: $hhl\ l = 2n + 1$
Space group: $P6_3/mmc$

Cell dimensions and intensities were measured on a Rigaku Denki computer-controlled four-circle diffractometer using monochromated Mo$K\alpha$ radiation with a graphite single crystal and a scintillation counter detector. Lattice constants were refined by a least-squares procedure using 35 2θ values. A crystal with dimensions $0.10 \times 0.10 \times 0.06$ mm was used for intensity measurement and was mounted on a glass fiber with an inclination to the c-axis in order to avoid the multiple diffraction. The linear absorption coefficient, μ, for Mo$K\alpha$ radiation is 62.4 cm^{-1}. Reflections hkl, $h \geqslant k \geqslant 0$ and $l \geqslant 0$, were measured over the section of the reciprocal lattice where the intensities of equivalent reflections change most gradually from the nearest one to the next. Integrated intensities were measured by the θ–2θ scan technique to a maximum 2θ of 100°. A scan range of ω for each reflection was calculated by the formula, $\Delta\omega = 1.2° + 0.5° \times \tan\theta$. Background was determined from 15-sec counts on both sides of the scan. Attenuators were automatically inserted when the maximum counting rate exceeded 5500 cps. Three standard reflections: (008), (220), and (060), were measured every 50 reflections during the data collection. They showed non-systematic drifts (their standard deviations were 0.55, 0.41, and 1.06%, respectively) during the experiment. Reflections of which the intensities were greater than two times their standard deviations were collected. The 331 independent reflections were collected and corrected for background and Lorentz-polarization factors, but the corrections for absorption and anomalous dispersion were not applied.

Structure Determination

A least-squares refinement of atomic parameters, which take the atomic parameters of the *BR* position of the mobile ion and of all the remaining aluminum and oxygen atoms of Tl–β-alumina as starting ones, gave an R value of 0.15 after 5 cycles of the refinement with the anisotropic temperature factors. The atomic position of rubidium atoms of the *aBR* and the *aBR′* positions were determined by calculating a three-dimensional Fourier systhesis of the stage of $R = 0.15$ and were included in the refinement using the anisotropic temperature factors. An R factor of 0.088 was obtained. The Fourier synthesis was calculated and the rubidium atom of the *mBR* position, situating at the midpoint along the way from the *BR* position to the *aBR* position, was found. The occupation parameters of the rubidium atom were then adjusted by integrating the electron density of the Fourier synthesis. The occupation parameters and other parameters were alternately refined step by step in the least-squares refinement. Although the atomic parameters of the rubidium atom of the *mBR* position were included in the calculation, it was finally clarified that the lowest R value was obtained by refining the atomic parameters of rubidium atom of *BR*, *aBR*, and *aBR′* position with those of other nonconducting ionic species. Thus, many atomic parameters may cause the parameter interaction. The final R value was 0.079. Although the *mBR* position was not used in the calculation for convenience, the Fourier synthesis of the stage of $R = 0.079$ is reliable as an experimental result because phase change (0 or π) of the structure factor, $F_0(hkl)$, rarely happens at this stage.

The final atomic and thermal parameters are listed in Table I. The negative values for the diagonal terms of the anisotropic temperature factors were obtained as in the case of Tl– and Ag–β-alumina. Rb–β-alumina was found to have the composition, $Rb_{2.6}Al_{22}O_{34}$, from the occupation parameters and to have the composition, $Rb_{2.3}Al_{22}O_{34}$, from the Fourier synthesis.

A complete list of the observed and calculated structure factors is shown in Table II. Atomic scattering curves taken from the International Tables for X-ray Crystallography were used throughout.

Description and Discussion of the Crystal Structure

A perspective drawing of the crystal structure is shown in Fig. 1. The crystal is formed

TABLE I

FINAL ATOMIC COORDINATES (×10⁴) AND THERMAL PARAMETERS (×10⁴)[a]

Atom	I	II	III	IV	x	y	z	β_{11}	β_{22}	β_{33}	β_{12}	β_{13}	β_{23}
Rb(*BR*)	2	*d*	$\bar{6}m2$	0.552	6667	3333	2500	80	321	5	160	0	0
					(0)	(0)	(0)	(22)	(88)	(2)	(44)	(0)	(0)
Rb(*BR'*)	6	*h*	*mm*	1.308	6909	3818	2500	−1	−5	2	−3	0	0
					(7)	(4)	(0)	(12)	(46)	(1)	(23)	(0)	(0)
Rb(*aBR*)	2	*b*	$\bar{6}m2$	0.010	0	0	2500	1318	5272	2374	2636	0	0
					(0)	(0)	(0)	(6113)	(24452)	(964)	(12226)	(0)	(0)
Rb(*aBR'*)	6	*h*	*mm*	0.732	8983	7966	2500	69	276	2	138	(0)	(0)
					(23)	(20)	(0)	(24)	(96)	(1)	(48)	(0)	(0)
Al(1)	12	*k*	*m*	12	8324	6648	1045	10	40	2	20	0	0
					(7)	(6)	(1)	(3)	(12)	(0)	(6)	(0)	(0)
Al(2)	4	*f*	$3m$	4	3333	6667	246	0	−1	1	0	0	0
					(0)	(0)	(3)	(7)	(26)	(1)	(13)	(0)	(0)
Al(3)	4	*f*	$3m$	4	3333	6667	1748	28	111	−3	56	0	0
					(0)	(0)	(3)	(8)	(32)	(1)	(16)	(0)	(0)
Al(4)	2	*a*	$\bar{3}m$	2	0	0	0	16	64	2	32	0	0
					(0)	(0)	(0)	(13)	(54)	(1)	(27)	(0)	(0)
O(1)	12	*k*	*m*	12	1572	3145	494	8	31	1	16	−1	−2
					(15)	(29)	(3)	(9)	(35)	(1)	(17)	(4)	(8)
O(2)	12	*k*	*m*	12	5023	46	1442	13	51	2	25)	2	4
					(22)	(0)	(3)	(7)	(28)	(1)	(14)	(4)	(9)
O(3)	4	*f*	$3m$	4	6667	3333	542	2	9	0	5	0	0
					(0)	(0)	(6)	(16)	(62)	(1)	(31)	(0)	(0)
O(4)	4	*e*	$3m$	4	0	0	1407	14	55	1	27	0	0
					(0)	(0)	(7)	(17)	(69)	(2)	(34)	(0)	(0)
O(5)	2	*c*	$\bar{6}m2$	2	3333	6667	2500	81	324	0	162	0	0
					(0)	(0)	(0)	(44)	(175)	(2)	(87)	(0)	(0)

[a] I, number of positions; II, Wyckoff notation; III, point symmetry; IV, number of atoms per unit cell. Estimated standard deviations are shown in parentheses. The y fraction is related to the x fraction with the equation $y = 2x$. Thermal parameters are in the form of $\exp[-(h^2\beta_{11} + k^2\beta_{22} + l^2\beta_{33} + 2hk\beta_{12} + 2hl\beta_{13} + 2kl\beta_{23})]$. $\beta_{22} = 4\beta_{11}$. $\beta_{12} = 2\beta_{11}$. $\beta_{23} = 2\beta_{13}$.

by the alternate stacking of the conduction layer of the rubidium ion and the spinel block, composed of the oxygen and the aluminum ions, along the c-axis infinitely. Two successive spinel blocks are covalently bonded by the corner-sharing $O_3Al–O–AlO_3$ tetrahedra along the c-axis and the common oxygen of the $O_3Al–O–AlO_3$ spacer column is located on the conduction plane, which is a mirror plane of the space group, $P6_3/mmc$. This space necessary for the movement of the rubidium ion is preserved by the column.

In the spinel block the oxygen ions are arranged in cubic-packing and the aluminum ions are located in the octahedral and the tetrahedral holes. The aluminum layer near the conduction plane consists of one kind of the aluminum ions with the octahedral coordinations. The aluminum layer located half way between successive conduction planes consists of two kinds of the aluminum ions with the octahedral and tetrahedral coordinations.

The unit lattice of β-alumina compounds is sensitive along the c-axis and insensitive along the a-axis according to the different properties of the binding within and between the layers. A unit lattice of Rb–β-alumina is found to be rather long along the c-axis as that of Tl–β-alumina among all the β-alumina compounds: It is longer by 0.38 and 0.34 Å along the c-axis

TABLE II

h	k	l	F_o	F_c	h	k	l	F_o	F_c	h	k	l	F_o	F_c
1	0	0	9.5	8.1	4	0	5	36.7	35.8	4	1	10	15.6	15.4
1	1	0	62.5	62.8	4	2	5	21.7	20.8	4	2	10	12.6	12.0
2	0	0	27.8	29.2	6	2	5	13.2	13.8	4	3	10	10.0	11.9
2	1	0	16.7	17.2	8	0	5	11.0	10.1	5	0	10	20.9	23.6
2	2	0	139.5	148.5	0	0	6	27.3	33.3	6	3	10	7.1	3.9
3	0	0	42.8	39.7	1	1	6	14.9	14.7	7	2	10	11.4	14.5
3	1	0	10.3	10.4	2	0	6	59.1	57.8	1	0	11	16.4	16.0
3	3	0	30.6	32.2	2	2	6	5.1	11.0	2	0	11	57.3	57.4
4	0	0	24.9	24.7	3	0	6	22.2	21.0	2	1	11	14.8	13.3
4	1	0	31.8	29.2	4	0	6	35.9	36.2	3	1	11	7.0	5.6
4	2	0	16.0	14.8	4	2	6	23.7	22.9	3	2	11	8.3	8.6
4	4	0	66.6	67.0	5	2	6	14.0	13.8	4	0	11	45.5	47.2
5	0	0	12.7	12.0	6	2	6	17.5	15.1	4	2	11	32.0	32.4
5	2	0	21.1	16.1	8	0	6	13.2	15.4	4	3	11	6.5	3.3
6	0	0	80.2	77.9	1	0	7	63.6	66.0	5	0	11	6.9	3.9
7	1	0	15.5	13.8	2	0	7	31.9	30.0	6	1	11	8.4	4.6
1	0	1	13.0	15.2	2	1	7	56.0	56.8	6	2	11	20.4	22.4
2	0	1	24.5	21.0	3	0	7	8.5	8.3	8	0	11	15.5	17.9
2	1	1	9.4	10.7	3	1	7	40.7	37.9	0	0	12	17.8	18.8
3	2	1	8.5	8.6	3	2	7	36.8	37.3	1	0	12	9.7	8.7
4	0	1	16.3	11.8	4	0	7	10.7	12.4	1	1	12	40.5	40.9
4	2	1	14.2	14.6	4	2	7	13.7	14.7	2	2	12	9.1	7.8
0	0	2	25.7	21.4	4	3	7	24.2	26.1	3	0	12	30.1	29.0
1	0	2	23.6	23.4	5	0	7	33.7	34.4	3	1	12	7.2	9.4
1	1	2	20.1	20.9	5	1	7	28.6	25.7	3	3	12	22.2	20.3
2	0	2	16.5	13.3	5	3	7	17.9	14.0	4	1	12	21.4	20.0
2	1	2	17.7	18.9	6	1	7	21.0	20.2	5	2	12	15.1	13.3
3	0	2	6.6	8.7	7	0	7	9.1	16.5	2	0	13	65.0	62.0
3	1	2	18.3	17.6	7	2	7	10.3	14.1	3	0	13	7.5	7.0
3	2	2	11.7	12.6	8	1	7	11.8	12.2	3	1	13	7.0	8.2
3	3	2	8.1	5.7	0	0	8	59.4	64.2	3	2	13	8.4	3.7
4	1	2	6.4	3.2	1	0	8	11.1	9.4	4	0	13	43.2	40.4
5	0	2	9.7	10.8	1	1	8	20.6	20.6	4	2	13	36.7	36.6
5	1	2	7.4	6.0	2	0	8	27.0	21.9	6	2	13	24.2	25.3
6	1	2	7.5	10.0	2	2	8	33.0	33.1	6	4	13	20.6	24.2
2	0	3	25.2	29.0	3	0	8	11.2	9.8	8	0	13	21.2	24.6
2	1	3	11.2	11.0	3	3	8	9.7	9.2	0	0	14	72.0	71.7
3	0	3	11.5	11.1	4	0	8	11.0	10.1	1	0	14	16.4	16.2
4	0	3	31.2	33.0	4	1	8	8.6	5.9	1	1	14	20.3	21.7
4	2	3	22.0	21.0	4	2	8	11.9	10.9	2	0	14	76.5	76.5
0	0	4	25.1	19.6	4	3	8	10.1	11.2	2	1	14	18.7	19.7
1	0	4	11.0	12.3	4	4	8	16.1	15.3	2	2	14	47.2	46.3
1	1	4	63.9	64.4	5	0	8	10.1	5.1	3	0	14	11.2	12.9
2	0	4	34.3	30.6	6	0	8	16.9	15.4	3	1	14	13.9	17.4
2	1	4	17.5	18.7	8	0	8	9.0	5.6	3	2	14	9.2	9.6
2	2	4	20.0	19.6	2	0	9	26.3	26.2	3	3	14	10.3	11.6
3	0	4	46.9	45.7	4	0	9	22.6	22.7	4	0	14	55.7	55.7
3	1	4	11.4	13.5	4	2	9	14.8	12.1	4	1	14	10.6	9.0
3	3	4	32.7	32.1	5	0	9	7.2	5.0	4	2	14	39.9	40.3
4	0	4	12.8	13.1	0	0	10	66.0	61.7	4	4	14	20.8	20.9
4	1	4	33.8	32.6	1	0	10	23.3	22.8	5	0	14	12.6	13.1
5	0	4	11.0	13.6	1	1	10	32.4	33.4	5	1	14	8.7	9.8
5	2	4	20.8	22.7	2	0	10	17.5	15.3	6	0	14	22.9	23.6
6	3	4	10.1	12.5	2	1	10	30.7	30.2	6	2	14	28.4	27.7
7	1	4	15.3	13.1	2	2	10	14.3	14.3	6	4	14	19.4	22.6
1	0	5	17.2	18.4	3	0	10	21.2	20.8	8	0	14	24.9	26.4
2	0	5	54.9	52.2	3	1	10	19.7	21.1	1	0	15	19.8	20.2
2	1	5	12.4	14.7	3	2	10	9.5	10.6	2	0	15	16.0	15.8
3	1	5	6.0	5.7	3	3	10	17.0	18.6	1	0	15	19.8	20.2
3	2	5	7.0	8.2	4	0	10	12.6	9.8	2	0	15	16.0	15.8

TABLE II (*continued*)

h	k	l	F_o	F_c	h	k	l	F_o	F_c	h	k	l	F_o	F_c
2	1	15	16.8	17.7	1	0	22	16.5	14.0	2	2	32	17.7	18.1
3	1	15	10.2	10.3	1	1	22	13.0	13.5	4	1	32	9.3	8.4
3	2	15	12.5	12.9	2	0	22	22.5	22.5	1	0	33	18.9	19.5
4	0	15	14.2	14.8	2	1	22	15.4	14.1	2	1	33	19.0	19.6
4	2	15	9.0	7.5	3	0	22	6.8	8.1	3	1	33	13.8	12.8
5	0	15	9.2	7.7	3	1	22	15.3	14.5	3	2	33	10.3	13.0
5	1	15	7.9	7.6	3	2	22	11.5	11.6	5	0	33	11.3	14.8
5	3	15	10.3	4.5	4	0	22	17.5	18.2	0	0	34	14.1	13.9
5	4	15	8.2	5.8	4	2	22	9.3	12.4	1	1	34	10.3	8.0
0	0	16	16.1	14.4	5	0	22	8.5	9.1	2	0	34	19.8	18.9
1	1	16	33.6	32.5	2	0	23	9.7	7.6	4	0	34	12.9	16.6
3	0	16	24.1	22.6	4	0	23	11.2	9.4	1	0	35	9.8	9.7
3	3	16	19.0	17.7	0	0	24	19.2	18.2	0	0	36	28.8	29.5
4	1	16	16.1	16.3	1	1	24	24.0	22.9	1	1	36	18.5	18.6
5	2	16	11.1	10.9	2	2	24	22.3	22.1	2	2	36	19.8	21.1
2	0	7	21.9	22.5	3	0	24	17.6	16.7	3	0	36	13.4	14.5
3	0	17	8.1	8.0	3	3	24	13.9	13.3	2	0	37	8.4	8.6
4	0	17	22.2	22.5	4	1	24	12.6	12.4	1	1	38	8.0	8.7
4	2	17	12.6	13.3	4	4	24	15.9	17.0	0	0	40	38.5	38.1
6	2	17	13.9	8.7	6	0	24	19.4	20.9	1	1	40	15.8	16.2
1	0	18	18.2	17.6	2	0	25	32.0	32.1	2	0	40	15.7	14.8
1	1	18	27.6	26.1	4	0	25	30.1	29.4	2	0	42	14.7	13.9
2	0	18	22.7	21.5	4	2	25	21.8	21.2	4	0	42	12.5	12.6
2	1	18	20.1	18.5	0	0	26	46.6	45.5	1	1	44	11.8	12.9
2	2	18	12.4	9.8	1	0	26	17.2	13.9	2	0	45	14.2	17.7
3	0	18	19.9	18.2	1	1	26	27.4	28.0	4	0	45	16.2	17.5
3	1	18	17.7	16.8	2	0	26	22.1	21.5					
3	2	18	13.4	13.1	2	1	26	17.7	16.8					
3	3	18	15.0	14.7	2	2	26	30.8	30.5					
4	0	18	15.5	15.5	3	0	26	22.2	21.7					
4	1	18	15.8	13.3	3	1	26	12.3	14.6					
4	2	18	15.5	16.2	4	0	26	17.3	17.9					
5	0	18	11.6	13.4	3	3	26	15.1	19.4					
1	0	19	24.6	24.1	4	1	26	13.1	17.8					
2	0	19	21.6	20.8	4	2	26	11.6	12.2					
2	1	19	19.5	20.9	6	0	26	18.6	18.3					
3	1	19	15.1	13.9	2	0	27	35.8	34.9					
3	2	19	15.4	16.2	4	0	27	26.2	26.0					
4	0	19	21.1	19.9	4	2	27	24.0	25.9					
4	2	19	12.3	11.8	0	0	28	52.6	50.3					
5	0	19	9.4	10.0	1	1	28	10.7	13.1					
5	1	19	10.6	9.0	2	2	28	34.5	34.9					
0	0	20	70.5	71.4	3	0	28	8.2	8.2					
1	0	20	18.3	17.3	6	0	28	19.8	21.5					
1	1	20	9.6	10.9	1	0	29	11.5	11.3					
2	1	20	10.4	8.7	2	0	29	9.3	7.6					
2	2	20	43.8	44.7	2	1	29	10.5	9.5					
3	2	20	10.3	14.4	5	1	29	8.2	3.2					
4	4	20	24.7	25.5	0	0	30	14.8	15.9					
6	0	20	24.7	26.4	1	0	30	8.3	10.3					
1	0	21	35.0	33.9	1	1	30	10.9	11.3					
2	1	21	30.1	29.5	2	0	30	8.8	4.8					
3	1	21	21.2	21.8	2	1	30	13.8	14.5					
3	2	21	22.6	23.9	3	1	30	8.8	11.4					
4	3	21	12.0	13.7	4	0	30	8.6	4.4					
5	0	21	13.8	17.2	5	0	30	13.9	13.7					
5	1	21	12.0	15.1	2	0	31	23.9	22.7					
5	3	21	13.0	9.8	4	0	31	19.3	21.6					
6	1	21	13.5	14.6	0	0	32	14.7	14.0					
0	0	22	12.4	9.4	1	1	32	14.0	15.0					

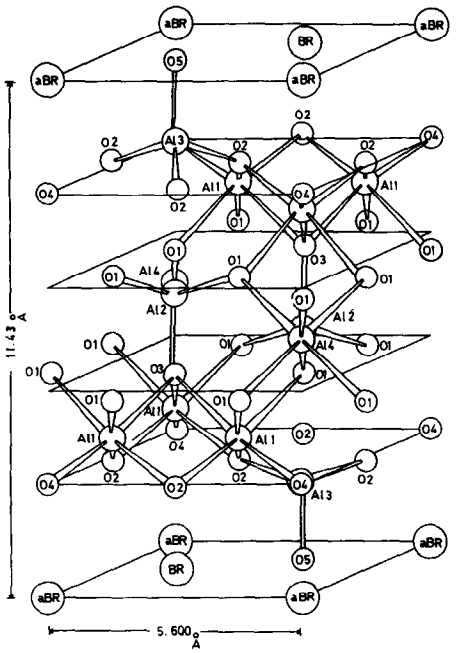

FIG. 1. A perspective drawing of the crystal structure to the *c*-axis.

than that of Ag– and Na–β-alumina (*3*, *4*). The spinel block has the almost equal volume for these compounds, but the covalently bonded O_3Al–O–AlO_3 column makes a remarkable contribution to the variation of the length of a unit lattice along the *c*-axis.

The distances between the oxygen atoms of different layers are listed in Table III for Rb–, Tl–, Ag–, and Na–β-alumina. In Rb–β-alumina about one-half of the elongation of a unit lattice along the *c*-axis is brought on by the elongation of the bond length between the O(5) atom, which is located on the conduction layer, and the Al(3) atom and the other half of the elongation is brought on by the expansion of the O(2)–Al(3)–O(5) angle with slightly elongated O(2)–Al(3) bond lengths. The observed values of these related structure parameters are listed in Table IV. The extreme distortion of the covalently bonded O_3Al–O–AlO_3 column is found in all β-alumina compounds, especially in Ag– and Na–β-alumina. This type of distortion might be a clue to understanding the ion conduction phenomena qualitatively. For example, the extreme contraction of the Al(3)–O(5) bond length might be explained as follows. The electron-attracting character of the O(2) atom is induced by the positive ionic character of the mobile ion of the *BR* site and so the double bond can be formed easily between the O(5) and the Al(3) atoms as one of the excited states as follows:

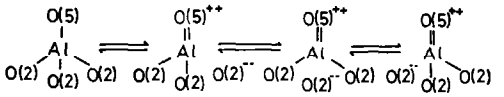

The electonegativity of the oxygen atom (3.5) differs greatly from that of the aluminum

TABLE III

PERPENDICULAR DISTANCES ALONG THE *c*-AXIS BETWEEN OXYGEN ATOMS OF DIFFERENT LAYERS

	Rb–β-alumina	Tl–β-alumina	Ag–β-alumina	Na–β-alumina
Ionic radii of the mobile ion (Å)[a]				
r_{M+}	1.48	1.44	1.26	0.95
Lattice constant (Å)				
a	5.600	5.608	5.595	5.594
c	22.87	22.96	22.49	22.53
Perpendicular distances along the *c*-axis				
between O(2)–*M*(*Br*)–O(2)′ atoms	4.84	4.84	4.63	4.65
O(4)–*M*(*aBR*)–O(4)′	5.00	5.05	4.82	4.84
O(3)–Al(1)–O(2)	2.06	2.06	2.06	2.06
O(1)–Al(1)–O(2)	2.17	2.20	2.17	2.18
O(3)–Al(2)–O(1)″	2.37	2.38	2.37	2.38
O(1)–Al(4)–O(1)″	2.26	2.25	2.26	2.26

[a] The ionic radii of the mobile ion were referred to those of Pauling.

TABLE IV

BOND LENGTHS AND ANGLES OF THE Al(3) TETRAHEDRON

	Rb-β-alumina	Tl-β-alumina	Ag-β-alumina	Na-β-alumina
Bond lengths (Å)				
O(5)-Al(3)	1.719(6)	1.720(6)	1.675	1.677
O(2)-Al(3)	1.782(4)	1.774(9)	1.762	1.768
Bond angles (°)				
O(2)-Al(3)-O(2)′	105.6(4)	105.5(5)	107.55	
O(2)-Al(3)-O(5)	113.2(4)	113.2(3)	111.33	

atom (1.5) and this causes the easy contraction of the single bond length, as in the case of C–F bond in the CF_4 compound (*5*). Therefore, the electron densities along the Al–O bonds are picked out as shown in Fig. 2. In Rb-β-alumina a slight double-bonding character appears, but in Tl-β-alumina it is apparent that the anisotropic temperature factors were used inadequately, so the bonding character of the Al(3)–O(5) bond is impossible to discuss.

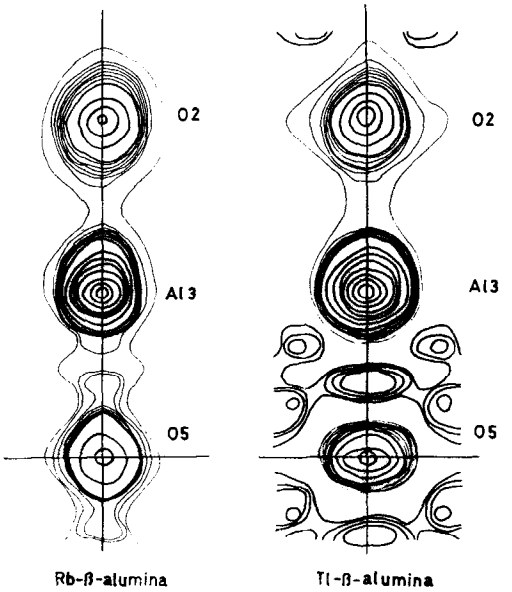

FIG. 2. The electron density along the O(5)–Al(3)–O(2) bond, in which the O(5)–Al(3)–O(2) bond was expanded as a straight line with each bond length. Thick solid contour lines were drawn at intervals of 10 electrons/Å^3. This solid contour lines were drawn at intervals of 1 electron/Å^3, the minimum value of which is 3 electrons/Å^3.

Bond lengths and angles are listed in Table V and are also shown in Fig. 3. No significant deviations of the bond lengths were observed in the spinel block from those of Tl–, Ag–, and Na-β-alumina.

The electron density at the conduction plane is shown in Fig. 4 for a series of β-alumina compounds and a perpendicular projection of the electron density along the conduction path to the *c* plane is shown in Fig. 5. The *BR*, *aBR*, *aBR′*, and *mBR* positions have electron densities of 175.8, 14.3, 19.8, and 12.2 electrons/Å^3, respectively. (The rubidium atoms have an electron density of 895.4 electrons/Å^3 when the *B* factor of the equation, $f = f_0 \exp(-B \sin^2\theta/\lambda^2)$, is zero.) As the electron density of the position with high symmetry tends to make a low peak as a peculiar character of the position, the positions with low peak densities cause doubt as to whether or not they are significant as the mobile ion site. The *mBR* position has higher electron density than that of Tl-β-alumina, and moreover, the low occupation of the *aBR* position is thought to be compensated by the occupation of the *mBR* position. Therefore the *mBR* position is correctly considered to be a mobile ion site. The occupation percentages of the mobile ion also can be calculated by using the occupation parameters. However, because the occupation parameters correlate with the thermal parameters, the information for the real occupation percentages of the mobile ion from the electron density is more reliable in this case.

TABLE V

BOND LENGTHS AND ANGLES OF Rb–, Tl–, Ag–, AND Na–β-ALUMINA[a]

	Number of bonds	Rb–β-alumina	Tl–β-alumina	Ag–β-alumina	Na–β-alumina
		Bond lengths			
Octahedral coordination					
Al(1)–O(1)	2	2.019(13) Å	2.026(12) Å	2.017 Å	2.022 Å
Al(1)–O(2)	2	1.841(10)	1.852(10)	1.839	1.837
Al(1)–O(3)	1	1.976(8)	1.966(9)	1.973	1.970
Al(1)–O(4)	1	1.824(8)	1.822(8)	1.821	1.819
Al(4)–O(1)	6	1.897(12)	1.899(12)	1.893	1.895
Tetrahedral coordination					
Al(2)–O(1)	3	1.800(14)	1.790(9)	1.806	1.801
Al(2)–O(3)	1	1.802(14)	1.814(15)	1.800	1.809
Al(3)–O(2)	3	1.782(8)	1.774(9)	1.762	1.768
Al(3)–O(5)	1	1.719(6)	1.720(6)	1.675	1.677
		Bond angles			
Octahedral coordination					
O(1)–Al(1)–O(2)		90.3(3)°	90.4(3)°	90.70°	
O(1)–Al(1)–O(3)		89.1(3)	89.2(3)	89.19	
O(1)–Al(1)–O(4)		84.4(3)	84.5(3)	84.04	
O(2)–Al(1)–O(3)		85.9(2)	86.2(4)	86.09	
O(1)–Al(4)–O(1)′		88.2(3)	88.7(3)	92.06	
O(1)–Al(4)–O(1)″		91.8(3)	91.3(3)	92.06	
Tetrahedral coordination					
O(1)–Al(2)–O(1)′		110.6(4)	110.6(4)	110.37	
O(1)–Al(2)–O(3)		108.4(3)	108.3(3)	108.56	
O(2)–Al(3)–O(2)′		105.6(4)	105.5(5)	107.55	
O(2)–Al(3)–O(5)		113.2(2)	113.2(3)	111.33	

[a] O(1)–Al(4)–O(1)′ expresses an angle made by two oxygens of the same layer and the aluminum. O(1)–Al(4)–O(1)″ expresses an angle made by two oxygens of different layers with each other and the aluminum.)

The mobile ion moves between successive *BR* positions by way of the *aBR* position. The *BR* position surrounded by six oxygen atoms has the highest occupation percentages through all the β-alumina compounds. In Rb–β-alumina, the metastable positions of the mobile ion, *aBR*, *aBR′*, and *mBR* positions, appeared in marked relief in the Fourier synthesis. The number of metastable positions appeared highest in Rb–β-alumina.

The atomic arrangement of the conduction plane with the oxygen atoms adjacent to the plane is shown in Fig. 6. All the stable positions of the mobile ion that appeared in the Fourier synthesis of Rb–β-alumina are also shown in this figure. The *BR* position is most stabilized in Coulomb potential energy and in the short-range Born–Mayer repulsive potential energy according to the results calculated by Wang *et al.* (*6*), which are shown in Fig. 7 for the ideal stoichiometric structure. The *aBR* position has the highest potential energy along the conduction path, but is most stable in polarization potential energy. The covalent property of the *aBR* position is also verified experimentally by photoelectron spectroscopy (*7*).

In Rb–β-alumina the *aBR′* position is stabilized next to the *BR* position as in Na–β-alumina. The *mBR* position, which is situated exactly on the midpoint along the conduction

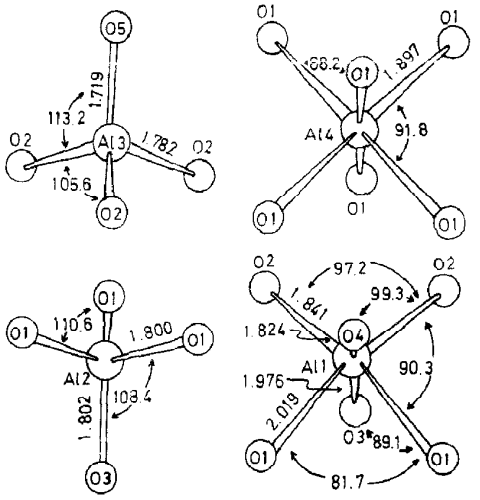

FIG. 3. Bond lengths and angles of the six-coordination and the four-coordination groups around the aluminum atom. The perspective direction is identical to that of Fig. 1.

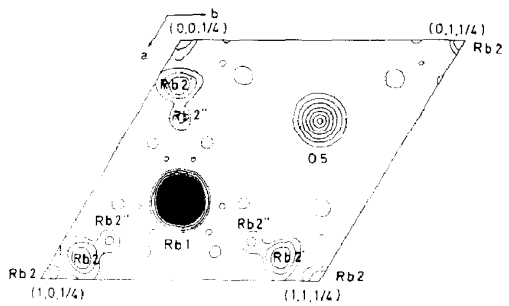

FIG. 4. The electron density in the conduction plane. Thick solid contour lines were drawn at intervals of 10 electrons/Å^3. Thin solid contour lines were drawn at intervals of 1 electron/Å^3, the minimum value of which is 4 electrons/Å^3.

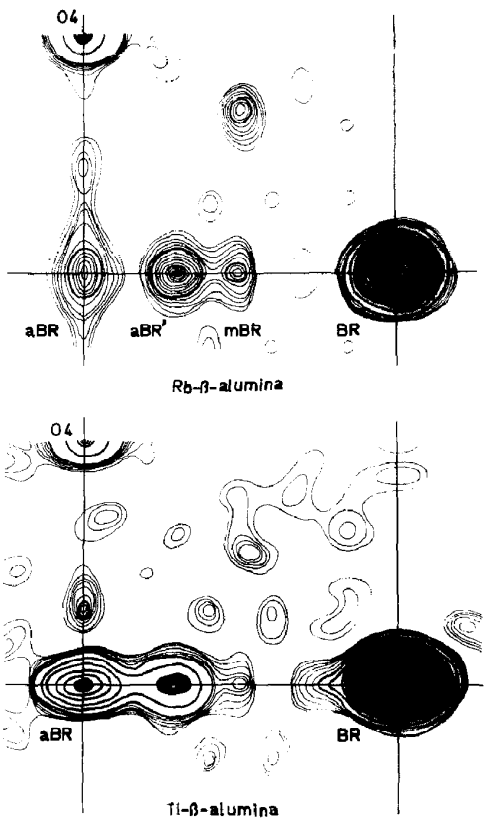

FIG. 5. A perpendicular projection of the electron density along the conduction path to the c-plane. Contour intervals are identical to those of Fig. 4.

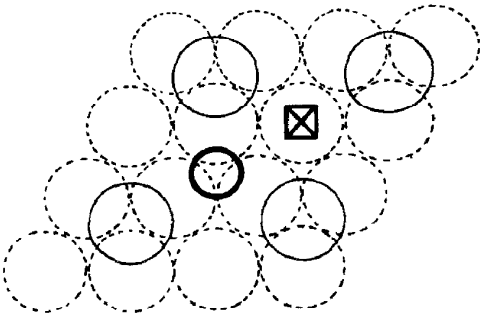

FIG. 6. The atomic arrangement of the conduction plane with the oxygen atoms adjacent to the plane as shown in (6).

path from the *BR* position to the *aBR* position, appeared in marked relief in Rb–β-alumina, although the *mBR* position has a nonzero electron density in Ag– and Tl–β-alumina. The *aBR'* position is thought to correspond to the minimum in potential energy near the 12 section of Fig. 7 and is thought to be stabilized in the Born–Mayer repulsive potential energy and also in polarization potential energy. The existence of two close minima in potential energy, that is to say, the *aBR'* and the *mBR* positions, is very interesting. Although the Born–Mayer repulsive potential energy makes a minimum slightly apart from

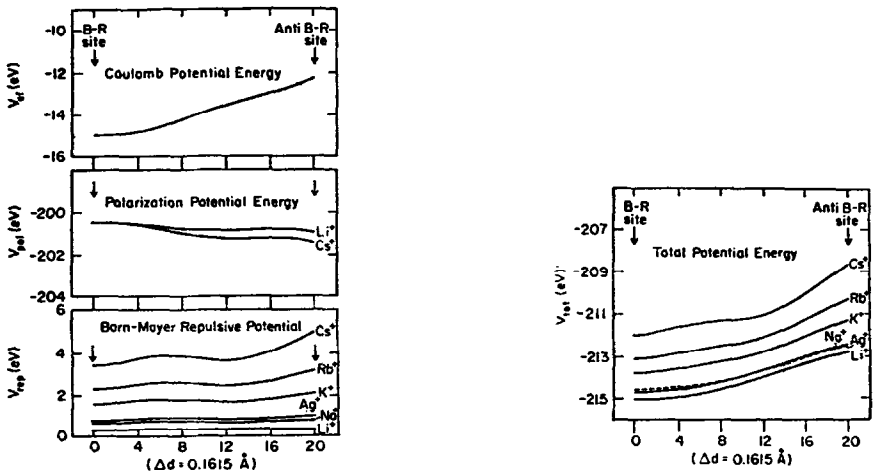

FIG. 7. The calculated potential energy maps along the conduction path by Wang, Gaffari, and Choi (*6*).

a midpoint to the *aBR* position on the conduction plane, the *mBR* position could be a minimum when the oxygen atom on the conduction plane is absent as a point defect or when the oxygen atom is displaced in the direction perpendicular to the conduction path in order to minimize the repulsive force. If the *mBR* position is meaningful as a rubidium site, the existence of two close minima in potential energy implies that there is need for an improved calculation of potential energy and/or that there are at least two kinds of correlated ionic movements on the conduction plane. Two close sites could have appeared in Fourier synthesis as the result of the geometrical average of the electron density over a crystal.

The extraordinary anisotropic vibrations of the atoms in the conduction plane were also observed as in the case of Tl–, Ag–, and Na–β-alumina, but were smaller in value.

Acknowledgment

Calculations were carried out on a HITAC 8700 computer at the Computer Center of the University using the Universal Crystallographic Computation Program System.

The authors wish to express their sincere thanks to Professor Yukimi Sasaki for his kindness and for our use of the diffractometer in his laboratory.

References

1. Y. Y. YAO AND J. T. KUMMER, *J. Inorg. Nucl. Chem.* **29**, 2453 (1967).
2. T. KODAMA AND G. MUTO, *J. Solid State Chem.* **17**, 16 (1976).
3. W. L. ROTH, *J. Solid State Chem.* **4**, 60 (1972).
4. C. R. PETERS, M. BETTMAN, J. W. MOORE, AND M. D. GLICK, *Acta Crystallogr.* **B27**, 1826 (1971).
5. L. PAULING, "The Nature of the Chemical Bond," Cornell Univ. Press, Ithaca, N.Y. (1960).
6. J. C. WANG, M. GAFFARI, AND S. CHOI, *J. Chem. Phys.* **63**, 772 (1975).
7. T. DICKINSON, A. F. POVEY, AND P. M. A. Sherwood, *J. Solid State Chem.* **13**, 237 (1975).